ISSN 0005-1179, Automation and Remote Control, 2025, Vol. 86, Nos. 1–4, pp. 1–17. © Pleiades Publishing, Ltd., 2025.

Performance Enhancement of Fuel Cell towards Sustainable Transport Using Optimized MPPT

A. Preethi[a],* and R. Arulmozhiyal[b],**

[a]*Vivekanandha College of Engineering for Women, Tiruchengode, Namakkal, TamilNadu, India*

[b]*Sona College of Technology, Salem, TamilNadu, India*

**e-mail: mpreethaa1@gmail.com*

***e-mail: arulmozhyali@sonatech.ac.in*

Received August 1, 2025; revised September 1, 2025; accepted October 15, 2025

Abstract—Fuel cells are emerging as a clean and efficient power source for electric vehicles (EV). But, due to their nonlinear characteristic nature, they are failed to maintain maximum efficiency. Standard MPPT algorithms often converge slowly and fluctuate around the maximum power point, which lowers overall energy use. To address these problems, this study proposes a modified long short-term memory (MLSTM) based controller for maximum power point tracking. This method uses predictive learning to estimate the maximum power point accurately and create adaptive control signals for the DC–DC converter. This ensures stable fuel cell operation and effective power delivery to the traction system. Simulation results demonstrate that the proposed approach achieved a tracking time of 0.57 s, THD of 9.66%, and efficiency of 99.25%, outperforming the conventional P&O method. The proposed controller not only improves the overall energy efficiency of the fuel cell system but also extends the driving range of the EV with renewable energy sources in hybrid vehicle architectures. This topology provides a promising solution to fuel cell based EV in terms of enhanced sustainability and efficiency.

Keywords: electric vehicle, MPPT, LSTM, modified LSTM, efficiency

DOI: 10.1134/S0005117925600892

1. INTRODUCTION

The early period of modern energy systems has utilized fossil fuels as the main energy source for various applications, like power generation and transportation [1, 2]. However, the rising demand for energy and greenhouse gas (GHG) emissions have grazed the search for cleaner and more sustainable energy source. Fuel cells have emerged as a promising solution to this issue. Unlike traditional internal combustion engines (ICEs), it provides higher efficiency and energy conversion with zero-emission., as the fuel cells generate electricity through an electrochemical reaction, it releases only water and heat as their byproducts. The International Energy Agency (IEA) states that the fuel cells, can play a major role in emission elimination particularly in transportation and power generation based systems. Figure 1 depicts the market proportionality of fuel cell based EVs.

Fuel cell electric vehicles (FCEVs) have gained significant attention as an alternative to battery electric vehicles (BEVs) and traditional ICE vehicles due to their fast refueling times and longer driving ranges. The FC utilized for reliable and clean power generation in turn reduces the dependence on fossil fuels. At the same time, they can adjust to different environmental conditions which makes them a superior sustainable energy source.

Similar to solar photovoltaic (PV) systems, fuel cells exhibit nonlinear current–voltag (I–V) characteristics, which denotes their power output varies based on operating conditions such as load demand, fuel supply and temperature. To maximize efficiency and energy extraction, maximum power point tracking (MPPT) techniques are employed to ensure the fuel cell operates at its optimal power point under changing conditions.

Over the years, MPPT topologies have moved on to artificial intelligence from basic empirical methods. Recent advances in artificial intelligence have introduced intelligent MPPT techniques, including ANN, fuzzy logic, and metaheuristic algorithms, which improve adaptability but face challenges such as heavy computational requirements and implementation complexity. Motivated by these limitations, this

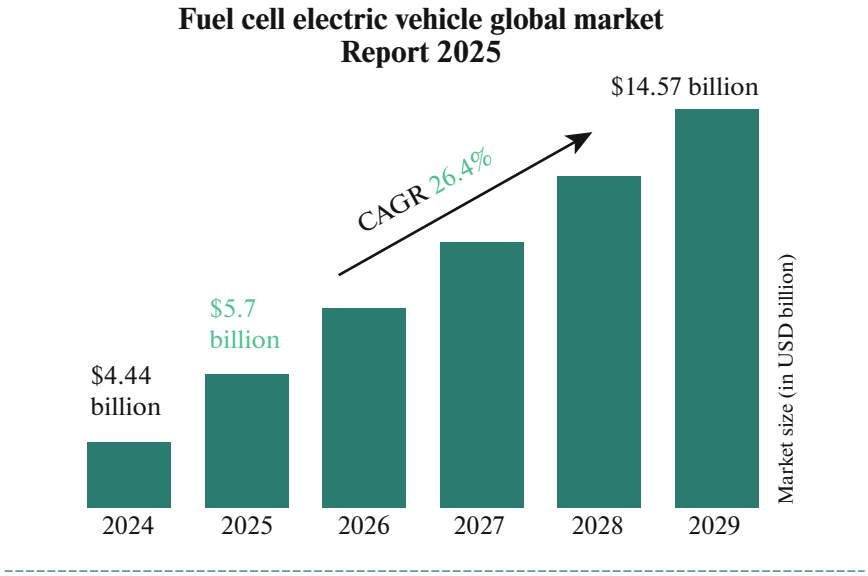


Fig. 1. Market for fuel cell based EV's.

research presents a novel modified long short-term memory (MLSTM) based mppt controller for FCEVs, addressing key challenges in efficiency, stability, and real-time adaptability.

Thus, key research contributions includes:

• Development of an intelligent MPPT approach utilizing MLSTM neural networks to accurately predict and track MPP of the fuel cell under dynamic operating conditions.

• Ensures optimal power extraction with reduced oscillations in voltage and current that typically occur in traditional MPPT techniques.

• Improves energy efficiency by dynamically adjusting the operating point based on real-time environmental and load conditions.

• Establishing the proposed method as a promising solution for EVs and hybrid renewable vehicle architecture.

2. RELATED WORKS

For the growing energy demand, Renewable power systems offer greater economic benefits compared to non-renewable energy sources. However, they exhibit stochastic behavior under varying peak load demand conditions. Additionally, factors such as energy storage limitations and battery size play a crucial role in establishing high-capacity renewable power generation systems. As a result, many power generation industries are shifting their focus toward hydrogen-based power systems [3].

The SOFS was formulated and analyzed under different water membrane conditions, where a ceramic electrolyte was positioned between the cathode and anode to facilitate electrochemical oxidation. This system offers several advantages, including high fuel flexibility, lower operating costs, the ability to function at elevated temperatures of up to 1000°C and high stability. Additionally, it produces minimal harmful gas emissions [4].

The molten carbonate fuel stack (MCFS) which operates at temperatures exceeding 600°C has been proposed. In this system, a molten carbonate salt mixture functions as the electrolyte, while non-precious metals serve as catalysts at both the cathode and anode. MCFS is known for its high efficiency, However, its drawbacks include the requirement for a large installation space, a relatively short lifespan, and significant carbon dioxide emissions.

Direct methanol fuel cells (DMFC) which are appropriate for portable applications has been discussed in [5–7]. However, DMFCs suffer from anode polarization, complex architecture and vulnerability to poisoning of carbon monoxide.

To mitigate these existing limitations, a proton exchange membrane fuel stack (PEMFS) is tailored to enhance the power delivery capacity with high operational efficiency. PEMFS offers several advantages, including lightweight design, rapid start-up, compact size, high operating speed, and excellent flexibility.

However, due its nonlinear I–V characteristics, the maximum power extraction becomes a challenging task. This challenge can be addressed through the implementation of MPPT controllers, which ensure optimal energy extraction from the fuel stack. The existing literature indicates that MPPT controllers have been developed using various approaches, including conventional, metaheuristic algorithms and AI networks [26]. Among conventional techniques, the P&O controller is most widely adopted, as it regulates power output between the fuel cell and the load under all temperature conditions [9].

A controller utilizing an artificial neural network (ANN) to effectively track the MPP with minimal oscillation, even under fluctuating temperature conditions has been proposed [10].

A strategy utilizing the salp swarm algorithm (SSA), for extracting the MPP from PEMFC has been developed [11]. The deviation between the estimated MPP voltage and the actual terminal voltage of the fuel cell is supplied to a PID controller, whose output adjusts the duty cycle of a boost converter to maximize power extraction from the PEMFC. A second-order sliding mode control (SMC) method was implemented for MPPT, while fuel cell pressure regulation was achieved using the super twisting algorithm (STA). The results demonstrated the effectiveness of the proposed control scheme, achieving an 85% reduction in oscillations. Furthermore, a hybrid PV–fuel cell system was modeled and simulated to evaluate its performance [12].

The enhanced slider MPPT technique has been developed for hybrid EV drive applications. It offers fast system response with reduced dependence on fuel cell operation. On the other hand, it caused high oscillations around MPP during dynamic temperature variations [13].

A control strategy of combined artificial bee colony (ABC) with fuzzy control (ABC-Fuzzy) has been introduced for PEMFC. It effectively maximized the output power, contributing significantly improvement in efficiency and extending its operational lifespan [14].

While the discussed MPPT strategies enhance efficiency, they also have limitations [15, 16]. ANN-based controllers require extensive training data and computational resources, making real-time implementation challenging. SSA and ABC-Fuzzy algorithms improve global optimization but may suffer from slow convergence and parameter tuning difficulties. The SMC-STA approach reduces chattering but increases implementation complexity. High oscillations around MPP under dynamic conditions remain a concern, impacting overall stability and efficiency.

To overcome this difficulties, the proposed work introduced a modified LSTM which can offer significant advantages over traditional MPPT techniques by efficiently capturing long-term dependencies in fuel cell power variations, leading to more accurate predictions.

Next to MPPT design, controller plays a vital role. The flyback converter applicable for both AC-DC and DC-DC power conversion has been formulated for FC. The key advantages of this converter include high energy storage, reduced noise, compact design and an efficient transient response [15]. However, its drawbacks include lower operational efficiency and substantial heat generation.

The push-pull power converter has been employed in hybrid PV/PEMFC power distribution networks to minimize switching losses and ensure a stable supply current [16]. However, it exhibits increased design complexity, while designing transformer for higher switching voltage.

To overcome the limitations of the half-bridge converter, a full-bridge isolated converter was employed to minimize output current ripples [17]. This converter offers advantages such as high efficiency, the ability to handle higher input voltage, reduced voltage stress and a lower requirement for passive components. However, its implementation comes with a high cost. Table 1 summarizes a some of the type of FC, MPPT topology and converters utilized in FC based EV.

From Table 1, it is inferred that the existing MPPT methods such as fuzzy logic, ANN, and hybrid AI improve tracking but still face challenges like slow convergence, high complexity, and limited adaptability. These drawbacks reduce stability and efficiency of fuel cell in EVs. This motivates the present study, which proposes a MLSTM based controller to address these gaps.

3. METHODOLOGY

Figure 2 illustrates a fuel cell electric vehicle (FCEV) drivetrain powered by a proton exchange membrane fuel cell (PEMFC).

Table 1. Summary MPPT controllers and their limitations summary of MPPT FC based EVs

Reference	Hybrid technology/system	MPPT/AI approach (controller)	Key features and innovations	Main drawbacks
[18]	PV/Wind/Fuel Cell Hybrid	Fuzzy Logic Controller-Based MPPT	Fuzzy logic MPPT for dynamic hybrid system	Fuzzy control parameter tuning is challenging; real-time adaptability may lag in extreme variations
[19]	PEMFS	Hybrid Bond Graph and Fuzzy Logic MPPT	Hybrid bond graph and fuzzy logic MPPT, experimental validation	Increased algorithm complexity; requires accurate modeling and may need significant computational resources
[20]	Fuel Cell	Various AI and Hybrid MPPT Methods	New hybrid MPPTs using AI for improved tracking and efficiency	May suffer from convergence issues and overfitting in AI models; Robustness to all operating ranges not always validated
[21]	PEMFS	Fuzzy Logic Controller-Based MPPT	Combines fuzzy control with multi-level boost for robust tracking and voltage regulation	Three-level topology can be more expensive; fuzzy rules need careful adaptation for different stacks
[22]	PV-Fuel Cell (Grid-Tied)	AI-Based MPPT	Grid integration with AI MPPT methods and converter performance analysis	Large systems can suffer from increased computational demand; grid synchronization added complexity unless designed properly
[23]	PEM Fuel Cell	ANFIS + Modified Manta Ray Algorithm (hybrid MPPT)	ANFIS-based MPPT with evolutionary optimization for high accuracy and fast response	ANFIS training requires substantial data; optimization methods may require retuning for different hardware

The MPPT controller optimizes power extraction by adjusting voltage and current to ensure maximum efficiency. A high gain boost converter steps up the fuel cell output voltage to a suitable level of a 3ϕ inverter, which converts DC to AC for driving the BLDC motor. The motor control unit receives Hall sensor FC signals and current feedback to regulate speed and torque efficiently. This system enables efficient energy conversion, ensuring smooth vehicle operation with enhanced fuel cell utilization.

3.1. PEMFC

A PEMFC is an advanced electrochemical energy conversion device that efficiently generates electricity using oxygen and hydrogen [24–26]. It is widely opted because of its high efficiency, quick start-up, lower operating temperature and zero-emission characteristics.

The PEMFC shown in Fig. 3 produces an electricity using an electrochemical reaction between oxygen and hydrogen, with water and heat as by products. The hydrogen molecules forms both protons and electrons. These produced electrons is utilized for electrical power generation and the protons pass through the PEM at the anode side. On the cathode side, both protons and electrons combine with oxygen and forms water, which ensures a clean and effective energy conversion process.

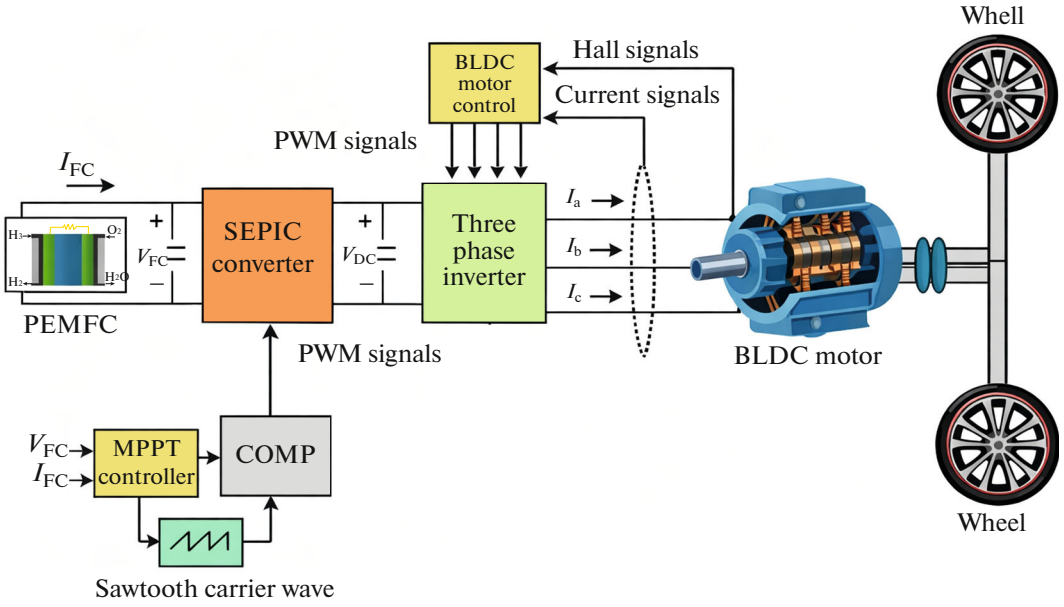


Fig. 2. Proposed architecture.

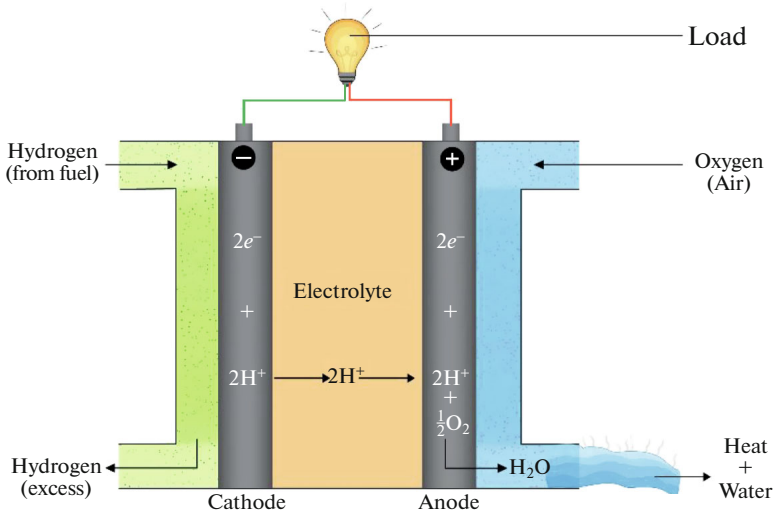


Fig. 3. Structure of the PEMFC.

3.2. Mathematical Model of PEMFC

The performance of a PEMFC can be expressed using mathematical equations related to its voltage, power, and efficiency.

3.3. Fuel Cell Voltage Equation

The output voltage of a PEMFC is given by

$$V_{FC} = E_{0ct} - V_{oh} - V_{ac} - V_{con}, \quad (1)$$

where E_{0ct}—open-circuit voltage; V_{oh}—Ohmic losses; V_{ac}—activation losses; V_{con}—concentration losses.

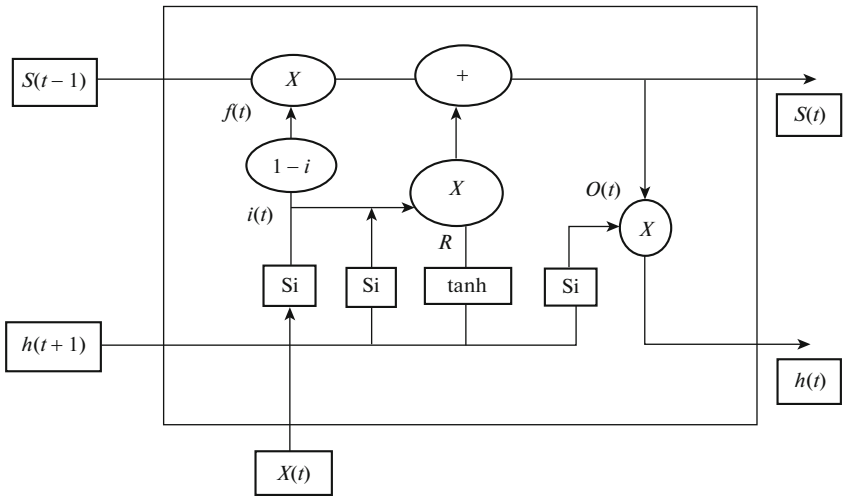


Fig. 4. Architecture of RNN-LSTM.

The open circuit voltage can be calculated as

$$E_{0\text{ct}} = 1.29 - 0.8e^{-3}\left(T_{\text{Fcope}} - 298.12\right) + 4.3e^{-5}\log\left(P_{\text{H}_2}\sqrt{P_{\text{O}_2}}\right)T_{\text{FCope}}. \quad (2)$$

3.4. MPPT Algorithm

MPPT is essential for FC to optimize their output power. Unlike PV systems, fuel cells exhibit nonlinear characteristics due to variations in temperature, reactant flow rate, and load demand. Traditional MPPT methods like P&O and Incremental Conductance (INC) suffer from slow convergence and instability under dynamic conditions [27, 28]. To address these challenges, a MLSTM based MPPT algorithm is proposed. Unlike traditional MPPT methods, LSTM processes time-series data, reducing steady-state oscillations and improving convergence speed [29–31]. It takes real-time inputs (voltage, current and temperature) to find the optimal duty cycle of the converter. By learning from historical trends, it enhances efficiency, minimizes power losses, and adapts to load variations. This approach significantly improves fuel cell performance and lifespan by preventing excessive power fluctuations. Further, to improve efficiency of LSTM, this work incorporated RNN with LSTM. By integrating LSTM with RNN, we retain the sequential learning capability of RNN while improving long-term memory for tracking the optimal fuel cell power point under varying conditions. Figure 4 shows the architecture of RNN-LSTM.

3.5. Working of RNN-LSTM

The given diagram in Fig. 4 represents a modified LSTM Cell, an advanced variation of the LSTM architecture used for sequential data processing. The operation of these circuit can be explained using the following equations:

$$i(t) = S_i\left(W_{xi}X_t + W_{hi}h_{t-1} + b_i\right), \quad (3)$$

$$f(t) = S_i\left(W_{xf}X_t + W_{hf}h_{t-1} + b_f\right), \quad (4)$$

$$g = \tanh\left(W_{xg}X_t + W_{hg}h_{t-1} + b_g\right), \quad (5)$$

$$(t) = S_i\left(W_{xo}X_t + W_{ho}h_{t-1} + b_o\right), \quad (6)$$

$$s(t) = S(t-1) * f(t) + i(t) * g, \quad (7)$$

$$h(t) = \tanh\left(s(t)\right) * o(t). \quad (8)$$

Removing the tanh activation function from the $h(t)$ equation, it improves the architecture's accuracy and significantly reduced the error rate.

New activation function called "LReLU-tanh" is utilized here.

The activation can be given as,

$$f(x) = \frac{2}{\left(1 + e^{-2f_{lr}}\right)} - 1, \tag{9}$$

where,

$$f_{lr}(x) = 1(x < 0)(\alpha x) + 1(x \geq 0)(x). \tag{10}$$

After modification, the architecture become

$$i(t) = S_i\left(W_{xi}X_t + W_{hi}h_{t-1} + b_i\right), \tag{11}$$

$$f(t) = (1 - i), \tag{12}$$

$$g = \tanh\left(W_{xg}X_t + W_{hg}h_{t-1} + b_g\right), \tag{13}$$

$$o(t) = S_i\left(W_{xo}X_t + W_{ho}h_{t-1} + b_o\right), \tag{14}$$

$$s(t) = S(t-1) * f(t) + i(t) * g, \tag{15}$$

$$h(t) = f_{lr}\left(s(t) * o(t)\right); \tag{16}$$

where $i(t)$—input gate; $f(t)$—forget gate; $s(t)$—cell state; $h(t)$—hidden state; $o(t)$—output state; S_i—sigmoid function.

While designing MPPT algorithm, fitness function plays a vital role. In this work, an multiobjective fitness function which optimizes the duty cycle of a DC-DC converter to ensure MPP from the fuel cell is formulated. It combines three function namely, power maximization, duty cycle prediction and minimizing LSTM prediction error. Thus, the formulated fitness function is

$$F(D) = \alpha\left|P_{\text{MPP}} - P(D)\right| + \beta\left|D_{k+1-D_k}\right| + \gamma E_{\text{LSTM}}, \tag{17}$$

where α, β, γ—weight factors; P_{MPP}—reference power; D_kD_{k+1}—previous and updated duty cycles; ELSTM—error predicted by the LSTM model.

This approach enhances MPPT tracking by reducing oscillations, improving response time, and ensuring efficient fuel cell operation. The integration of real-time optimization with LSTM-based learning makes it superior to traditional MPPT techniques.

3.6. Algorithm of the Proposed MPPT

1. Initialize weights and biases, $s(t)$ and $h(t) = 0$.
2. Acquire real-time fuel cell data.
3. $X(t) = [V, I, P, T]$.
4. Split data for training and testing.
5. Compute forget gate using Eq. (4).
6. Input gate computation using Eq. (11).
7. Generates new memory updates using Eq. (13).
8. Update cell state using Eq. (15).
9. Compute output gate using Eq. (14).
10. Update hidden state using Eq. (16).
11. Compute instantaneous power.
12. Compute duty cycle error.
13. Compute hybrid fitness function using Eq. (17).

Table 2. The parameter configuration of RNN-LSTM

Topology	Parameter
Number of LSTM Layers	3
Activation function	Sigmoid
Optimizer	Adam
Learning rate	0.001
Loss function	Cross-entropy

14. Update LSTM weights using gradient descent.

15. Repeat until convergence occurs.

This modified LSTM-based MPPT algorithm with multiobjective optimization ensures faster, more efficient, and stable power tracking for fuel cells.

The parameter configuration of RNN-LSTM is tabulated in Table 2.

3.7. Boost Converter (SEPIC Converter)

Fuel cells generate variable DC voltage, which can fluctuate based on load conditions and fuel availability. Since SEPIC can step up the input voltage while maintaining a regulated output, it ensures stable power delivery to loads. Additionally, it provides continuous input current, reducing stress on the fuel cell and minimizing ripple and EMI. Its low voltage stress on components also enhances efficiency and lifespan, making it ideal for fuel cell-powered systems. So it is more suitable for FC applications compared to traditional boost converters (Fig. 5).

The voltage gain of the circuit is represented in Eq. (18)

$$V_0 = \frac{D}{1-D} V_{\text{in}}. \tag{18}$$

3.8. Voltage Source Inverter (VSI)

A VSI shown in Fig. 6 is commonly used to drive brushless DC (BLDC) motors, providing precise control over motor speed and torque. The standard VSI topology for BLDC motors consists of a three-phase inverter bridge with six switches, typically implemented using insulated gate bipolar transistors (IGBTs) or MOSFETs. This configuration enables efficient electronic commutation by sequentially activating the switches based on rotor position feedback, often obtained from Hall sensors.

3.9. BLDC Motor

Brushless DC (BLDC) motors (depicted in Fig. 7) are integral to electric vehicles (EVs) due to their high efficiency, converting up to 96.5% of electrical energy into mechanical energy, thereby extending

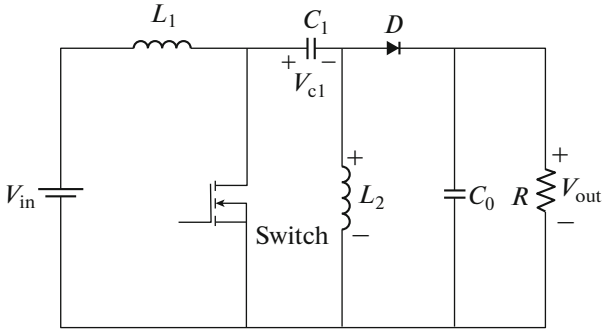


Fig. 5. SEPIC converter.

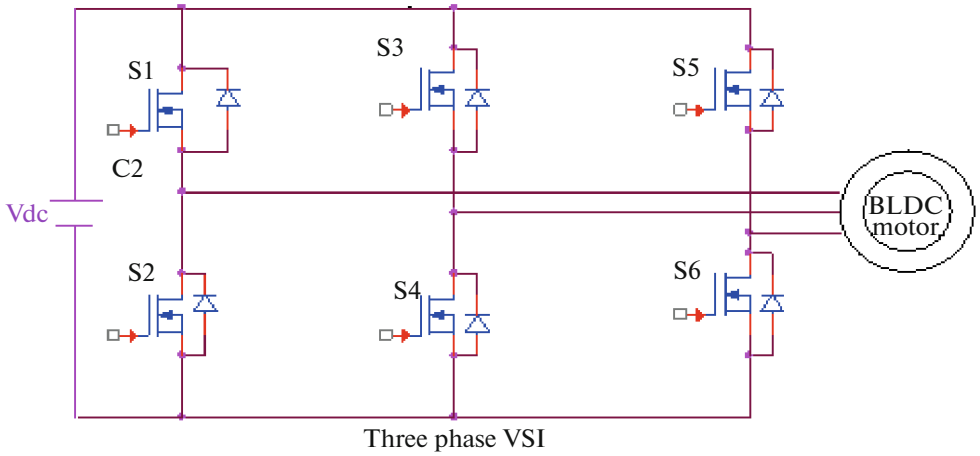


Fig. 6. VSI for BLDC motor.

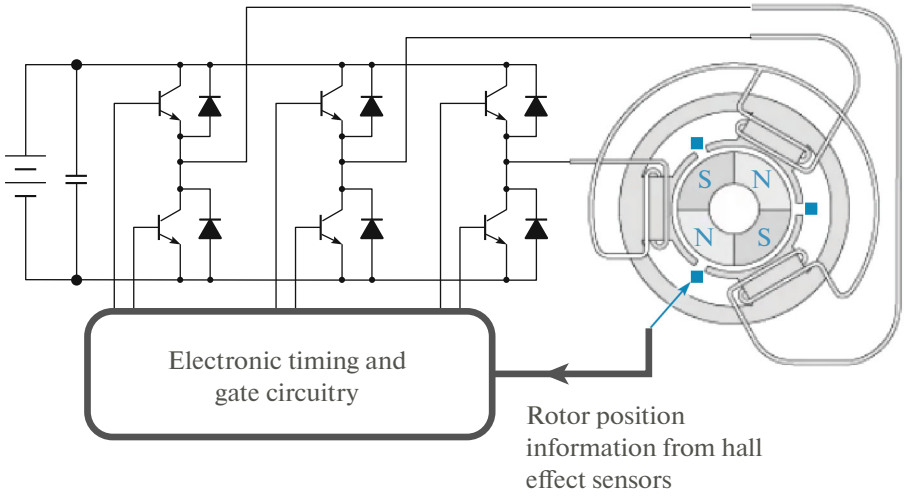


Fig. 7. BLDC motor drive.

driving range. Their quiet operation enhances passenger comfort by reducing noise and vibration. The absence of brushes minimizes mechanical wear, leading to lower maintenance needs and increased reliability. Additionally, BLDC motors' precise speed and torque control contribute to the responsive performance of EVs. These attributes make BLDC motors a preferred choice in the advancement of electric mobility [32–34].

It operates on the principle of electronic commutation, eliminating the need for mechanical brushes. It consists of a stator with electromagnets and a rotor with permanent magnets. An electronic controller sequentially energizes the stator windings based on the rotor's position, creating a rotating magnetic field that interacts with the rotor's magnetic field, producing torque and causing rotation. This method reduces friction and wear, enhancing efficiency and extending the motor's lifespan. Precise control of the stator's magnetic field allows for accurate speed and torque regulation, making BLDC motors suitable for applications requiring high performance and reliability. Controlling a three-phase inverter is essential for the efficient operation of BLDC motors is incorporated using SPWM which aims to generate a smooth sinusoidal current by modulating the width of the voltage pulses supplied to the motor. By adjusting the duty cycle of these pulses, the inverter can produce a more continuous and smooth rotation, reducing torque ripple and electromagnetic interference.

4. RESULTS AND DISCUSSION

In recent years, integrating fuel cells with BLDC motors has emerged as a promising approach to developing efficient and sustainable EV. Fuel cells, especially PEMFCs, offer high energy density and zero

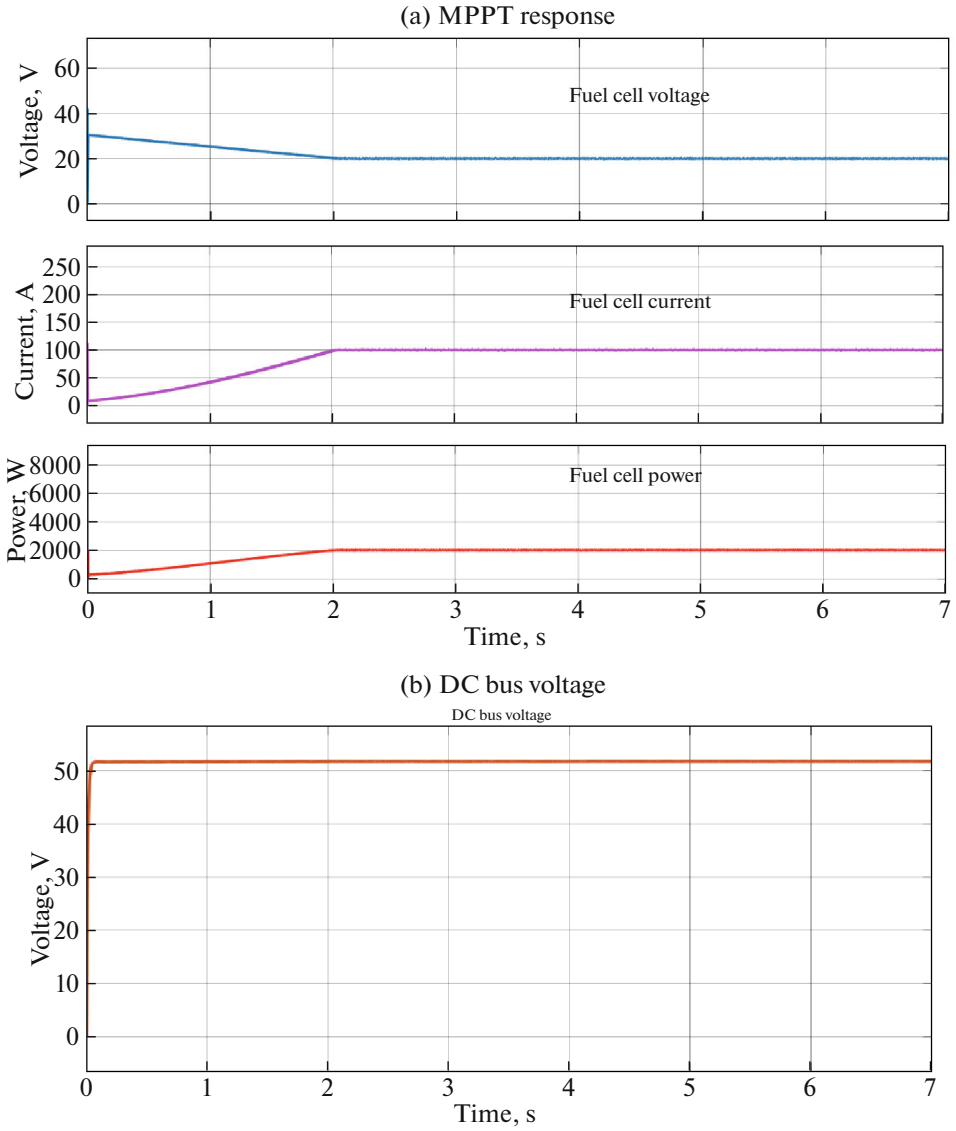


Fig. 8. Performance of P&O algorithm.

emissions, making them ideal candidates for clean energy applications. When combined with BLDC motors, the resulting system can significantly enhance the performance of EV's.

This section delves into the outcomes of implementing a fuel cell-powered BLDC motor drive system. The insights gained from this analysis aim to highlight the potential benefits and address the challenges associated with adopting fuel cell-based propulsion systems in modern EV's. Table 3 depicts the design parameters of the proposed fuel cell system.

4.1. Performance Analysis

The performance analysis of a FC with MPPT controller is analyzed under two different cases.

Case 1. Under normal operating condition.

Case 2. Variation in pressure.

Case 1. Under normal operating condition (under the ideal pressure range).

In order to analyze the effectiveness of the proposed MPPT algorithm, the proposed system is examined using two algorithms, traditional P&O and proposed RNN-LSTM algorithm. Figure 8 depicts the performance of P&O algorithm.

(c) Motor characteristics

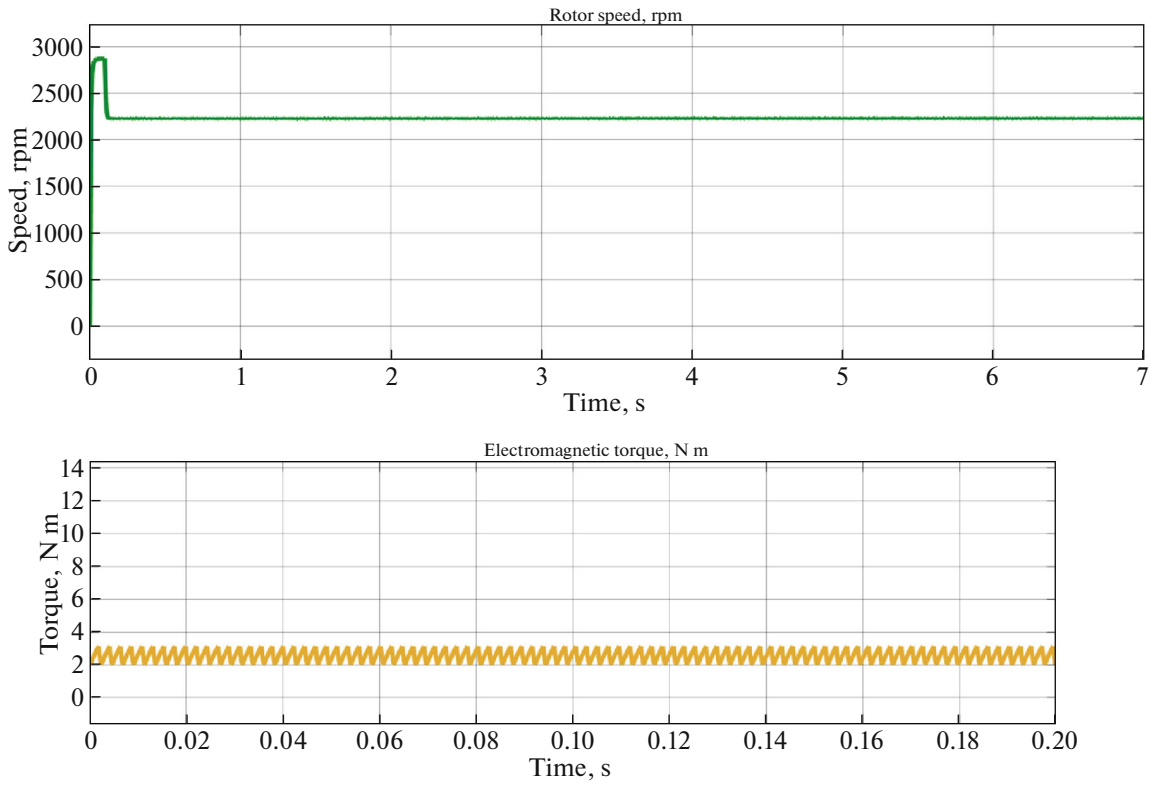


Fig. 8. (Contd.)

Figure 8a represents P&O MPPT tracking for a fuel cell system. Initially, the voltage decreases, while the current increases, indicating the system's attempt to track the MPP. The power output rises steadily, showing that the algorithm successfully adjusts the operating point to extract maximum power. The stabilization of voltage, current, and power after 2 s suggests that the P&O algorithm has effectively converged to the MPP. Figure 8b shows the DC bus voltage. Figure 8c depicts speed and torque of the BLDC motor.

Figure 9a represents RNN-LSTM based MPPT tracking for a fuel cell system. The fuel cell system exhibits a transient response at the start, followed by stable operation. The voltage initially fluctuates but

Table 3. Design parameters of the proposed fuel cell system

Constraints	Values
Selected power of the fuel stack	2 kW
Oxygen pressure in partial condition	1.00 bar
Hydrogen pressure at the partial condition	1.500 bar
Overall utilized fuel cells (N)	65.0
Voltage of fuel cell stack at open circuit state	65 V
Voltage of fuel cell at peak power point (VMPP)	45.0 V
Current of the fuel cell at peak power point (IMPP)	133.33 A
Basic air passing rate (Ipm)	506.40
Constant value of gasses (R)	84.092, J mol^{-1} K^{-1}
Constant of faraday (F)	95 432.218, C mol^{-1}
Composition levels of fuel cell	99.95%
The consumption level of oxygen	59.3%

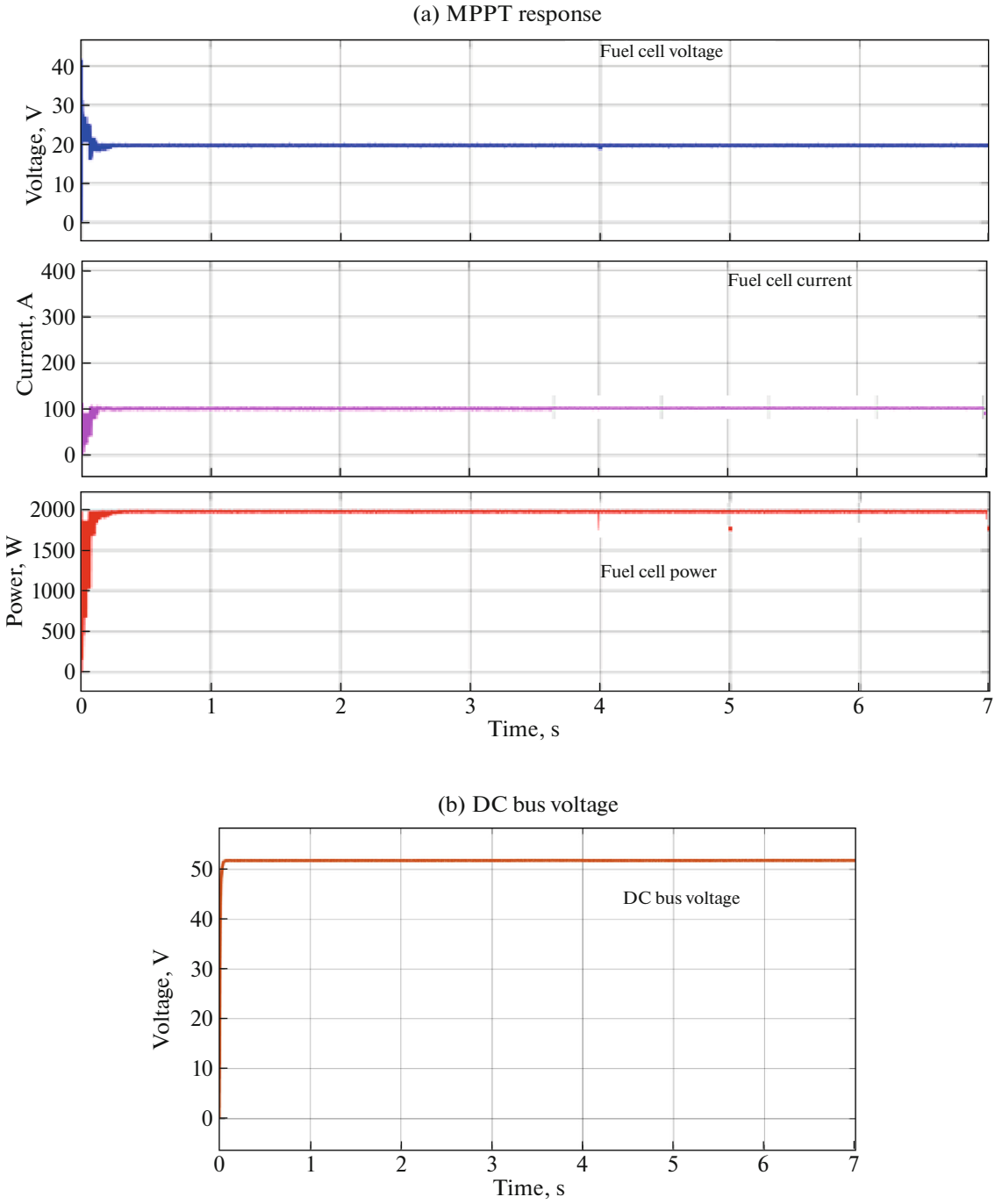


Fig. 9. Performance of RNN-LSTM algorithm.

settles quickly, indicating effective regulation. The current and power rise sharply before reaching a steady-state, suggesting efficient power tracking. Overall, the system achieves stable power generation with minimal oscillations after the initial transient phase. Figure 9b indicates the dc bus voltage which quickly stabilizes around 54 V, indicating effective voltage regulation. From Fig. 9c, it is observed that the electromagnetic torque initially experiences a sharp peak and then stabilizes at around 2.5 N m. This indicates a transient response at startup, followed by a steady-state operation. The system effectively regulates torque, minimizing fluctuations after the initial surge. This behavior suggests efficient motor control with rapid stabilization.

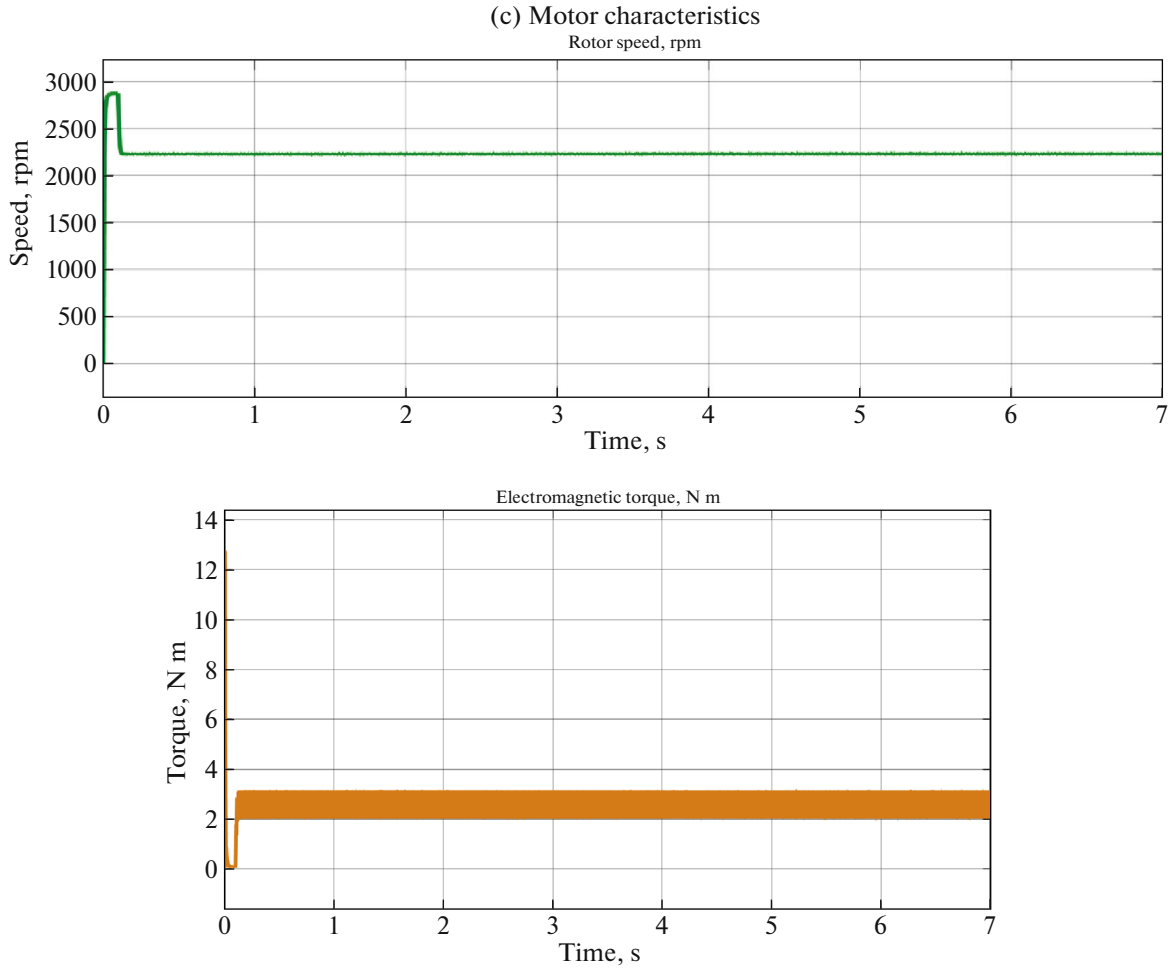


Fig. 9. (Contd.)

Case 2. Variation in pressure.

A step change in fuel cell pressure is introduced in MATLAB to observe its variations after 4 s.

From Figs. 10 and 11, it is observed that P&O illustrate the variations in fuel cell voltage, current, and power over time. The voltage exhibits a gradual decline and the current steadily rises, indicating an increasing power requirement, with a noticeable dip around 4 s, due to a step change in fuel cell pressure. Similarly, the power output follows an increasing trend but experiences a transient drop at the same time as the current dip, before stabilizing. This system eventually stabilizes, indicating its ability to recover from disturbances. Whereas in case of RNN-LSTM, the voltage remains relatively stable with minor fluctuations, suggesting steady operation. Thus, P&O takes some more time to stabilize its tracking, whereas RNN-LSTM exhibits more stable operation with improved regulation. The transient effects are minimized, ensuring smoother performance. Hence, it can be concluded that the proposed RNN-LSTM based MPPT exhibits higher stability.

4.2. Power Quality Analysis

Figure 12 shows total harmonic distortion (THD) analysis for a BLDC motor drive. A lower THD value, as seen in (b) compared to (a), indicates improved power quality and reduced torque ripple in BLDC motors. High THD can lead to excessive motor heating, increased losses, and acoustic noise. In contrast, the lower THD of 9.66% in RNN-LSTM suggests better motor performance, smoother operation, and higher efficiency.

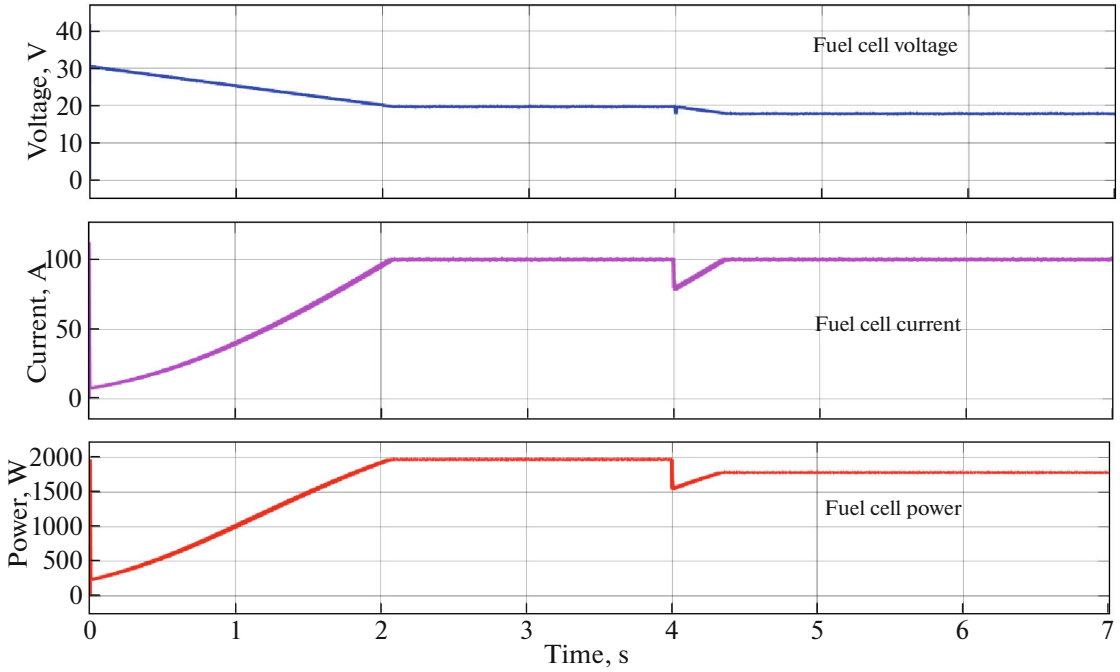


Fig. 10. Performance of P&O algorithm.

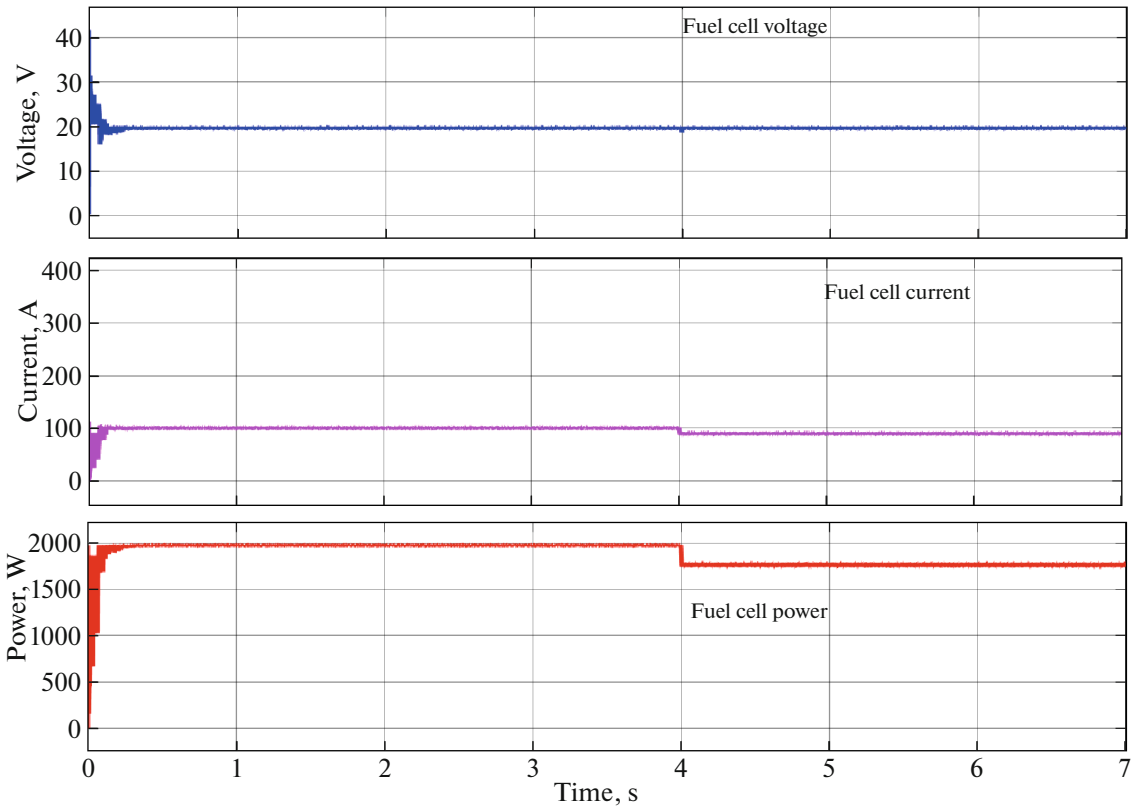


Fig. 11. Performance of RNN-LSTM algorithm.

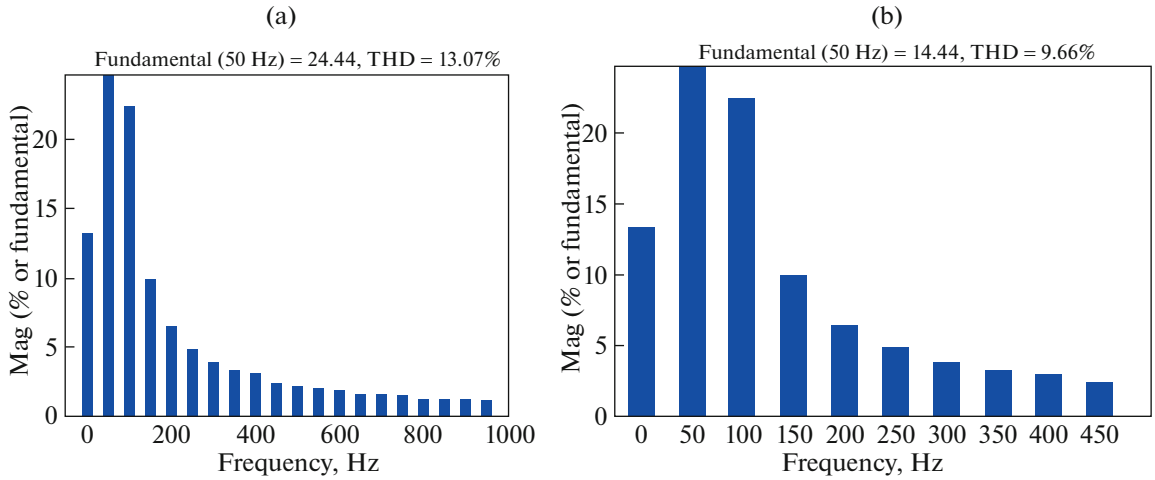


Fig. 12. THD analysis (a) system with P&O (b) RNN-LSTM MPPT.

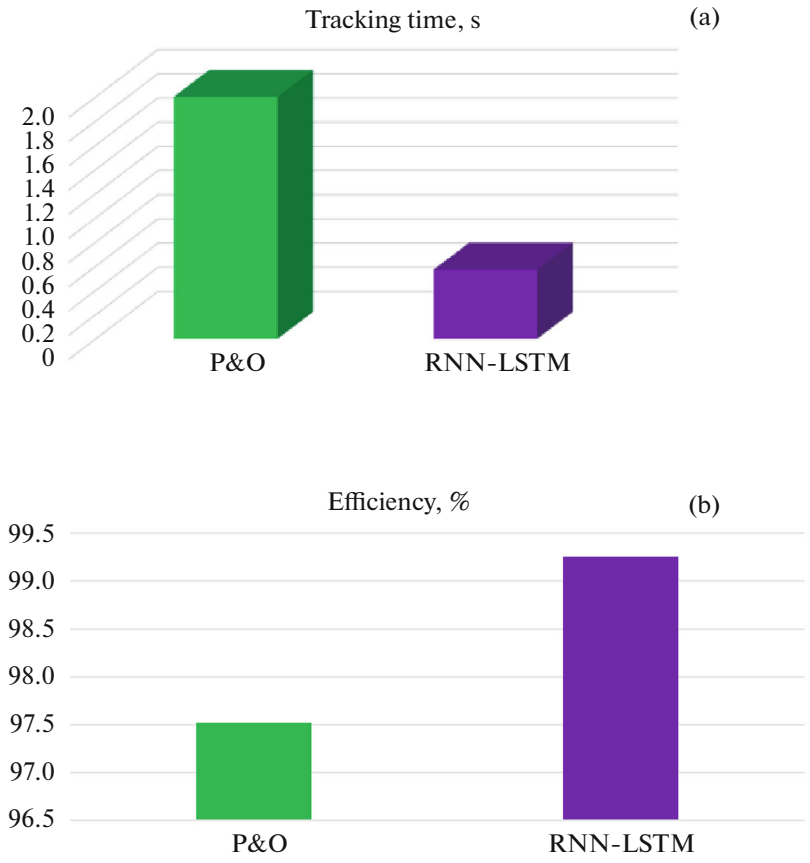


Fig. 13. Performance analysis of control algorithms: (a) tracking time, s, and (b) efficiency, %.

4.3. Comparative Analysis

From Table 4 and Fig. 13, it is observed that the P&O method tracks the MPP in 2 s with an efficiency of 97.52%, whereas RNN-LSTM achieved 99.25% efficiency, an improvement of 1.73% over P&O, while reducing tracking time by 71.5%. This indicates that RNN-LSTM achieved faster convergence and higher efficiency compared to P&O at dynamic conditions. The improved tracking speed ensures minimal power loss, making it more suitable for real-time applications. Overall, RNN-LSTM proves to be a more efficient and responsive MPPT technique.

Table 4. Comparison of performance of control algorithms

Techniques	Tracking time (s)	Efficiency (%)
P&O	2	97.52
RNN-LSTM	0.57	99.25

5. CONCLUSIONS

This study proposed a modified LSTM-based MPPT controller for fuel-cell electric vehicle applications. Comparative evaluation with the conventional P&O algorithm demonstrated that the modified LSTM achieved faster convergence (0.57 s), higher efficiency (99.25%), and reduced oscillations compared to P&O. The controller also improved power quality, with a lower THD of 9.66%, ensuring smoother BLDC motor performance. These results confirm that the proposed approach enhances stability, efficiency, and energy utilization in fuel-cell systems, facilitating their integration into electric and hybrid vehicle architectures. Further research may focus on real-time hardware implementation of the controller, extending its application to larger hybrid renewable systems, and optimizing the algorithm for reduced computational demand in embedded platforms.

AUTHOR CONTRIBUTION

Conceptualization, A. Preethi, R. Arulmozhiyal; Methodology, A. Preethi; Investigation, R. Arulmozhiyal; Resources, A. Preethi, R. Arulmozhiyal; Writing, A. Preethi.

FUNDING

This work was supported by ongoing institutional funding. No additional grants to carry out or direct this particular research were obtained.

CONFLICT OF INTEREST

The authors of this work declare that they have no conflicts of interest.

REFERENCES

1. Meenalochini, P., Priya, R.A., Pugalenthi, R., and Jagadeeshwaran, A., *J. Energy Storage*, 2024, vol. 80, p. 110255.
2. Jagadeeshwaran, A. and Kumar, H.S., in *Wind and Solar Energy Applications*, CRC Press, 2023, pp. 59–79.
3. Nayak, A.K., Ganguli, B., and Ajayan, P.M., *Energy Rep.*, 2023, vol. 9, pp. 3508–3530.
4. Ghoshal, S., Banerjee, S., Mahato, C.K., and Chanda, C.K., in *2022 Second International Conference on Advances in Electrical, Computing, Communication and Sustainable Technologies (ICAECT)*, IEEE, 2022, pp. 1–6.
5. Szcześniak, A., Milewski, J., Szabłowski, Ł., Bujalski, W., and Dybiński, O., *Energy*, 2020, vol. 200, p. 117442.
6. Ferguson, S. and Tarrant, A., *Front. Energy Res.*, 2021, vol. 9, p. 668431.
7. Alias, M.S., Kamarudin, S.K., Zainoodin, A.M., and Masdar, M.S., *Int. J. Hydrogen Energy*, 2020, vol. 45, no. 38, pp. 19620–19641.
8. Basha, C.H. and Rani, C., *Soft Comput.*, 2022, vol. 26, no. 13, pp. 6021–6040.
9. Ge, Z., Wu, L., Zhang, F., and He, Z., *J. Power Sources*, 2015, vol. 297, pp. 260–264.
10. Rafikiran, S., Devadasu, G., Basha, C.H., Tom, P.M., Prashanth, V., Dhanamjayulu, C., Kumbhar, A., and Muyeen, S.M., *Energy Rep.*, 2023, vol. 9, pp. 5826–5842.
11. Fathy, A., Abdelkareem, M.A., Olabi, A.G., and Rezk, H., *Int. J. Hydrogen Energy*, 2021, vol. 46, no. 8, pp. 6087–6099.
12. Souissi, A., *Energy Rep.*, 2021, vol. 7, pp. 3390–3399.
13. Kanouni, B. and Mekhilef, S., *Int. J. Hydrogen Energy*, 2022, vol. 47, no. 4, pp. 2685–2707.
14. Fan, L., and Ma, X., *Sci. Rep.*, 2022, vol. 12, no. 1, p. 4316.
15. Goudarzian, A., Khosravi, A., and Raeisi, H.A., *Eng. Sci. Technol. Int. J.*, 2022, vol. 26, p. 101007.
16. Musumeci, S. and Di Mauro, S., in *6th International Conference on Clean Electrical Power (ICCEP)*, IEEE, 2017, pp. 541–548.
17. Wei, Y., Luo, Q., and Mantooth, A., in *IEEE Workshop Wide Bandgap Power Devices Applications in Asia (WiPDA Asia)*, IEEE, 2020, pp. 1–6.

18. Khan, M.J. and Mathew, L., *Neural Comput. Appl.*, 2019, vol. 31, no. 10, pp. 6331–6344.
19. Badoud, A.E., Mekhilef, S., and Ould Bouamama, B., *Arab. J. Sci. Eng.*, 2021, vol. 46, no. 8, pp. 6087–6099.
20. Safarishaal, M. and Sarvi, M., *AIP Adv.*, 2023, vol. 13, no. 4, p. 0144806.
21. Hai, T., Alazzawi, A.K., Zhou, J., and Farajian, H., *Int. J. Hydrogen Energy*, 2023, vol. 48, no. 11, pp. 4430–4445.
22. Reddy, B.R.S., Reddy, V.V., and Kumar, M.V., *Electr. Power Syst. Res.*, 2023, vol. 216, p. 109053.
23. Ali, Z.M., Al-Dhaifallah, M., Al-Gahtani, S.F., and Muranaka, T., *Control Eng. Pract.*, 2023, vol. 134, p. 105481.
24. Parekh, A., *Front. Energy Res.*, 2022, vol. 10, p. 956132.
25. Mallick, N. and Mukherjee, V., *Int. J. Hydrogen Energy*, 2020, vol. 45, no. 53, pp. 29271–29287.
26. Basha, C.H., Mariprasath, T., Murali, M., and Rafikiran, S., *Mater. Today Proc.*, 2022, vol. 52, pp. 290–295.
27. Younas, U., Kulaksiz, A.A., and Ali, Z., *IEEE Access*, 2024, vol. 12, pp. 77032–77047.
28. Divya, G., *Lib. Prog. Libr. Sci. Inf. Technol. Comput.*, 2024, vol. 44, no. 3.
29. Gozhyj, A., Nechakhin, V., and Kalinina, I., Enhancing solar panel efficiency with LSTM-based MPPT controllers, *Doctoral Dissertation*, Germany, 2024.
30. Oliver, J.S., David, P.W., Balachandran, P.K., and Mihet-Popa, L., *Sustainability*, 2022, vol. 14, no. 12, p. 7205.
31. Srivani, S.G., Rao, P.N., Srinivasulu, V., Bhavana, R., and Appanna, A.L., in *7th International Conference on Computation System and Information Technology for Sustainable Solutions (CSITSS)*, IEEE, 2023, pp. 1–6.
32. Mandre, P., Somanna, B., Gupta, S., and Nema, S., in *IEEE International Students' Conference on Electrical, Electronics, and Computer Science (SCEECS)*, IEEE, 2023, pp. 1–6.
33. Sangeetha, B., Manjunatha, K., Thirusenthil Kumaran, P., Sheela, A., Yamuna, K.S., and Sivakumar, S., *Arch. Comput. Methods Eng.*, 2024, vol. 31, no. 3, pp. 1507–1518.
34. Nagarathinam, E., Devaraju, B., Jayamoorthy, K., Radhakrishnan, P., Chandra Mohan, S.L., Perumal, V., and Balakrishnan, K., *Energy Eng.*, 2024, vol. 121, no. 8, pp. 2129–2142.

Publisher's Note. Pleiades Publishing remains neutral with regard to jurisdictional claims in published maps and institutional affiliations.
AI tools may have been used in the translation or editing of this article.